ACS chemical biology

ARTICLES

pubs.acs.org/acschemicalbiology

Small Molecule Inhibition of the TNF Family Cytokine CD40 Ligand through a Subunit Fracture Mechanism

Laura F. Silvian,[†,*] Jessica E. Friedman,[†] Kathy Strauch,[†] Teresa G. Cachero,[†,⊥] Eric S. Day,[†] Fang Qian,[†] Brian Cunningham,[‡] Amy Fung,[‡,∥] Lihong Sun,[†] Lihe Su,[†] Zhongli Zheng,[†,#] Gnanasambandam Kumaravel,[†] and Adrian Whitty[§,*]

[†]Department of Drug Discovery, Biogen Idec, 12 Cambridge Center, Cambridge, Massachusetts 02142, United States

[‡]Sunesis Pharmaceuticals, Incorporated, 341 Oyster Point Boulevard, South San Francisco, California 94080, United States

[§]Department of Chemistry, Metcalf Center for Science and Engineering, Boston University, 590 Commonwealth Avenue, Boston, Massachusetts 02215, United States

Supporting Information

ABSTRACT: BIO8898 is one of several synthetic organic molecules that have recently been reported to inhibit receptor binding and function of the constitutively trimeric tumor necrosis factor (TNF) family cytokine CD40 ligand (CD40L, aka CD154). Small molecule inhibitors of protein−protein interfaces are relatively rare, and their discovery is often very challenging. Therefore, to understand how BIO8898 achieves this feat, we characterized its mechanism of action using biochemical assays and X-ray crystallography. BIO8898 inhibited soluble CD40L binding to CD40-Ig with a potency of IC_{50} = 25 μM and inhibited CD40L-dependent apoptosis in a cellular assay. A co-crystal structure of BIO8898 with CD40L revealed that one inhibitor molecule binds per protein trimer. Surprisingly, the compound binds not at the surface of the protein but by intercalating deeply between two subunits of the homotrimeric cytokine, disrupting a constitutive protein−protein interface and breaking the protein's 3-fold symmetry. The compound forms several hydrogen bonds with the protein, within an otherwise hydrophobic binding pocket. In addition to the translational splitting of the trimer, binding of BIO8898 was accompanied by additional local and longer-range conformational perturbations of the protein, both in the core and in a surface loop. Binding of BIO8898 is reversible, and the resulting complex is stable and does not lead to detectable dissociation of the protein trimer. Our results suggest that a set of core aromatic residues that are conserved across a subset of TNF family cytokines might represent a generic hot-spot for the induced-fit binding of trimer-disrupting small molecules.

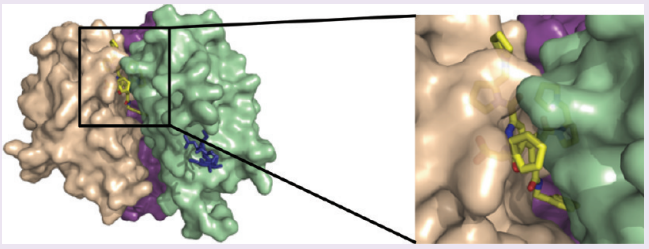

Obtaining small molecule (*i.e.*, synthetic organic) inhibitors against protein−protein interactions (PPI) is a major current challenge in chemical biology and drug discovery.[1−4] Despite many attempts involving a wide range of PPI targets, if special cases such as integrins, proteinases, and GPCRs are excluded, then only a relatively small number of PPI inhibitors have been reported, and with the exception of some complex natural products,[5] in only a handful of cases has a synthetic inhibitor of a classical PPI interface progressed as far as clinical trials.[6−8] Improving this historically low success rate would potentially render tractable a large number of biologically compelling PPI targets. Because relatively few PPI inhibitors have been reported, each new example adds to our knowledge of how ligand binding and inhibition can be achieved in such systems. This is particularly true for inhibitors of constitutive — rather than transient — PPI, which present a distinct challenge [9,10] and for which few well-characterized inhibitors exist.[11,12]

The TNF family cytokine CD40 Ligand (CD40L) is a compelling target for inhibition by a small molecule. This is because although it is located on the external surface of the cell, it has proven intractable to targeting by protein therapeutics for reasons that a small molecule inhibitor might circumvent. CD40L is expressed on activated T cells, B cells, and a number of other cell types and signals through interaction with CD40, a 45 kDa type I membrane receptor located primarily on B-cells, monocytes, and macrophages.[13] A number of antibodies that block the CD40L/CD40 interaction, such as hu5c8, have reached clinical trials in autoimmune diseases including lupus nephritis,[14] alloislet graft rejection, [15,16] and atherosclerosis.[17] When present in stoichiometric excess, the hu5c8 Fab fragment binds at three identical symmetry-related epitopes on the CD40L trimer.[18] The antibody binds at a site that overlaps the expected CD40 binding site at each of the three subunit interfaces of CD40L.[19] Clinical trials with these anti-CD40L antibodies on autoimmune patients have been halted, however, due to thromboembolic complications.[20] The cause of these adverse events is not fully known but has been

Received: January 28, 2011
Accepted: March 18, 2011
Published: March 18, 2011

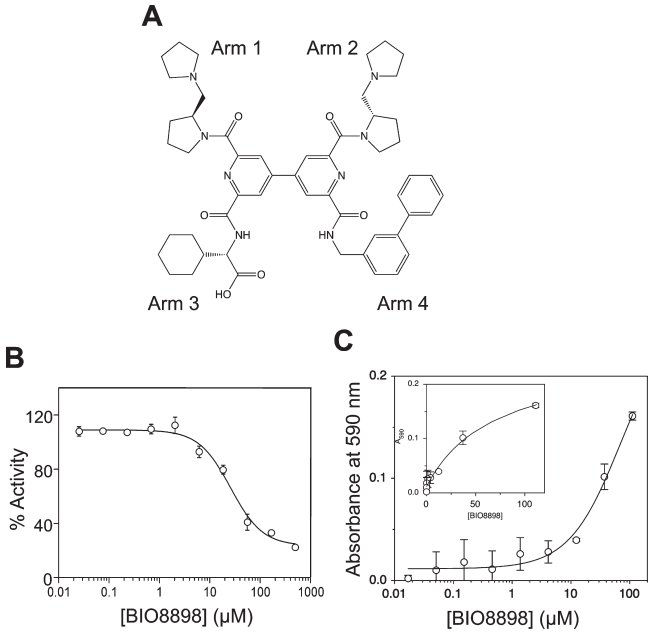

Figure 1. Structure and activity of BIO8898. (A) Chemical structure of BIO8898. (B) BIO8898 inhibits the binding of 40 ng mL^{-1} mycCD40L to CD40-Ig with an IC_{50} of 25 μM. CD40-Ig was coated on the assay plate, and the binding of mycCD40L was measured after 1 h by DELFIA using a europium-labeled antimyc antibody, as described in Methods. Data points are the average of triplicate measurements from a single experiment, with the standard deviation shown by the error bars. The solid line represents the best fit of a hyperbolic (single site) binding equation. (C) BIO8898 inhibits the ability of 3 ng mL^{-1} mycCD40L plus 50 μg mL^{-1} cyclohexamide to induce apoptosis in BHK cells transfected with a chimeric receptor comprising the extracellular domain of CD40 fused to the transmembrane and cytoplasmic domains of the structurally related TNF family receptor TNFR2, or p75. The number of viable cells present after 2 days was determined by MTT staining, as described in Methods. The absorbance of control wells containing the same concentration of DMSO but no BIO8898 was subtracted from each measurement. A higher absorbance at 590 nm indicates more live cells. Data are plotted as the average of two independent experiments, with the error bars showing the spread between the values observed in each experiment. Inset plot shows the same data plotted on a linear rather than a logarithmic concentration axis. The BIO8898 dose–response curve does not reach saturation because the compound concentrations was limited by poor solubility at the low DMSO levels that the assay can tolerate. The solid line represents the best fit to a hyperbolic binding equation (EC_{50} = 69 μM).

proposed to involve Fc cross-linking or effector functions of the antibodies.[21] If so, this undesirable activity could be circumvented by a small molecule inhibitor, potentially resulting in a more favorable safety profile.

Several small molecule inhibitors of the CD40L/CD40 interaction have been reported recently. Suramin, a polyaromatic bisnapthylamine trisulfonic acid that shows immunosuppressive activity,[22] was first reported to inhibit TNFα/TNFR interactions.[23,24] It was shown by gel filtration and by biochemical measurements to function by disrupting the trimeric structure of TNFα, though no structural information exists to show how trimer disruption is achieved. More recently, Suramin has been shown to also inhibit CD40L binding to CD40 and indeed in biochemical binding assays and B-cell proliferation assays does so with 30-fold higher potency compared to its inhibition of TNFα/TNFR.[25] Subsequently, a variety of other polyaromatic compounds have been reported to inhibit the CD40L/CD40 interaction with micromolar affinities,[26,27] including the food-colorant erythrosine, which is a promiscuous inhibitor of protein–protein interaction interfaces.[28] These reports suggest that this interface is druggable by small molecule inhibitors. Understanding whether these compounds, or smaller fragments derived from them, might represent viable starting points for drug discovery against CD40L and, if so, how they might be optimized to improve their affinity and selectivity would be greatly aided by knowledge of the mechanism of action of these inhibitors on CD40L, which has not previously been determined.

We report here the characterization of a small molecule inhibitor of CD40L, designated BIO8898,[29] that exemplifies a novel mode of action for a PPI inhibitor. A high-resolution co-crystal structure of the inhibitor–target complex shows that BIO8898 acts by disrupting the structure of the constitutively trimeric CD40L molecule. The compound intercalates between two subunits, accessing the core of the trimer and disrupting its native, 3-fold symmetry. This mechanism of action of BIO8898 is reminiscent of the trimer disruption mechanism that was recently reported for the trimeric cytokine TNFα,[12] though there are also important differences. Our results suggest that trimer disruption represents a generic mechanism for inhibition of TNF family cytokines, and potentially also other constitutively oligomeric proteins, by small molecule inhibitors. Indeed, on the basis of the topology of the CD40L/BIO8898 complex we propose that some constitutive PPI complexes might, counterintuitively, be easier to inhibit with a small molecule than are lower affinity, transient PPI interfaces.

RESULTS AND DISCUSSION

Biochemical Characterization. BIO8898 (Figure 1A) was reported several years ago as a discovery resulting from screening a compound library for the ability to bind to CD40L,[29] as detected by mass spectrometry after rapid separation from unbound library members by gel filtration.[30] Because small molecule inhibitors of PPI targets such as CD40L are rare and potentially of interest as drug leads, we further characterized the activity of BIO8898 to establish its mechanism of action.

The compound, synthesized as described in the Methods (see also Supplementary Figure S1), inhibits CD40L activity in assays measuring receptor binding and also functional activity. Figure 1B shows that BIO8898 inhibits the binding of myc-tagged soluble CD40L (mycCD40L) to an assay plate coated with a CD40-Ig fusion protein comprising the extracellular domain of CD40 fused to the hinge, CH2, and CH3 domains of human IgG1. Binding of mycCD40L to the plate was measured by dissociation enhanced lanthanide fluorescence immunoassay (DELFIA),[31] using a europium-labeled antimyc antibody as detection reagent. In this assay, BIO8898 inhibited CD40L binding with a concentration giving 50% inhibition (IC_{50}) of ~25 μM. The activity of BIO8898 in a cellular context was also evaluated, using a baby hamster kidney (BHK) cell line stably transfected with a chimeric receptor comprising the extracellular domain of CD40 fused to the transmembrane and cytoplasmic domains of the structurally related TNF family receptor TNFRp75. In this assay, ligation of CD40 by CD40L causes cell death through apoptosis mediated by the TNFRp75 death domain.[32] Cell viability after 2 days was measured by MTT staining. In viable cells MTT (3-(4,5-dimethylthiazol-2-yl)-2,5-diphenyltetrazolium bromide) is enzymatically reduced by

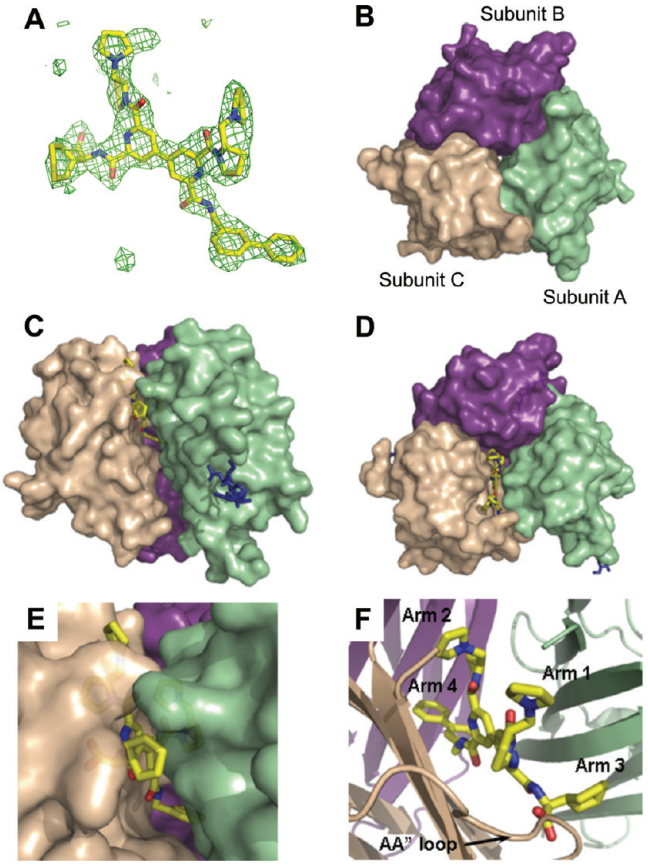

Figure 2. Structure of BIO8898/CD40L complex. (A) Sigma-A weighted omit map density contoured around BIO8898 at 1 sigma. (B) Space-filling representation of native CD40L trimer, as viewed from the top in relation to the 3-fold axis of symmetry, to compare with BIO8898-bound CD40L: subunit A (green), subunit B (magenta), subunit C (tan). (C) Side view and (D) top view of the complex of BIO8898 with CD40L. The atoms of the inhibitor are colored as follows: C, yellow; N, blue; O, red. The atoms of the CD40L glycan that were visible in the structure are shown in stick representation (dark blue), and the subunits are colored as in panel B. (E) Closer view of the inhibitor binding region from panel C with protein subunits A and C rendered partially transparent to better show the orientation of the bound compound and the extent to which it is buried within the protein. (F) Closer view of the inhibitor binding region, with CD40L subunits shown in ribbon representation to illustrate the binding locations of the four arms of the bound BIO8898.

the mitochondrial respiration pathway, generating a dark blue formazan product that can be quantified as a measure of the number of living cells.[33] Figure 1C shows that BIO8898 inhibits CD40L-induced apoptosis in this assay in a dose-dependent manner. The dose−response in the assay does not reach saturation because the highest dose at which BIO8898 could be tested (111 μM) was limited by the compound's solubility at the very low DMSO levels tolerated by this assay. Nevertheless, the potency observed in the apoptosis assay is within ~3-fold of the 25 μM IC_{50} seen Figure 2B, which is entirely in keeping with the somewhat lower potency that is often observed in cellular assays *versus* biochemical inhibition assays. This result establishes that BIO8898 inhibits the interaction of CD40L with CD40 in a cellular context, and thus its activity in Figure 2B is not an artifact of the CD40-Ig construct or the assay format used for the inhibition assay.

The biochemical activities of compounds with low potencies such those observed for BIO8898 in Figure 2B and C can result from a variety of assay artifacts including promiscuous aggregation-based inhibition.[34,35] We therefore attempted to co-crystallize the compound with CD40L to establish whether it possessed a distinct and robust binding mode that would validate it as a *bona fide* "hit" and, if so, to derive clues concerning how binding occurs in this case and how the potency of the compound might be improved. To maximize site occupancy by the weak-binding BIO8898, CD40L (100 μM) was crystallized with 1 mM compound, representing a large excess over both the protein concentration and the K_D for their interaction (presumed to be less than or equal to the IC_{50} value of 25 μM from Figure 1B). The resulting crystal diffracted to a resolution of 2.5 Å, and the structure was solved by molecular replacement using native CD40L as a search model, followed by domain-independent rigid body refinement.

Structure of the Complex. The structure revealed the surprising result that, although native CD40L is constitutively homotrimeric (Figure 2B) and contains three identical receptor binding sites,[36] each CD40L trimer binds only a single molecule of BIO8898. Clear difference density was observed at 2.5 sigma levels at 2.5 Å resolution. The compound was placed into density, and its orientation was unambiguous in the complex despite its quasi-symmetrical four-armed structure. An unbiased sigma-A weighted omit map in which refinement was performed in the absence of compound indicates that the compound binds in only one orientation (Figure 2A). Most surprisingly, BIO8898 binds not to the surface of the protein but rather intercalates between two subunits in the CD40L trimer, accessing the core of the protein and disrupting its native 3-fold symmetry (Figure 2C−E). The small molecule binds between the hydrophobic surfaces of the interface between two subunits, designated A and C, with one 2-(*N*-pyrrolidinomethyl)pyrrolidine substituent directed toward the solvent (Arm 1) while the second projects toward the interior core of the trimer (Arm 2; see Figures 1A and 2F). The 2-cyclohexyl-2-aminoacetic acid substituent (Arm 3) points toward solvent but is covered by the CD40L AA″ loop, comprising residues Tyr145, Tyr146, and Met148 of monomer C, protecting the hydrophobic surface of this substituent from exposure to solvent. The carboxylate group on Arm 3 interacts with the protein through direct and water-mediated hydrogen bonds with the backbone amides, as described below. The remaining, 2-aminomethylbiphenyl substituent (Arm 4) of the compound projects deep into the CD40L trimeric core. The position occupied by Arm 4 in the core of the protein makes it impossible for more than one compound to bind per trimer due to steric occlusion. On the basis of calculations of interface buried surface area using ProtorP v. 1.0,[37] the buried protein surface area of CD40L contacting BIO8898 totals 485 $Å^2$, which is approximately one-quarter of the total surface area that is buried at the interface between two subunits in unbound CD40L (974 $Å^2$ per subunit = 1950 $Å^2$ buried surface area).

The induced cleft that forms the binding site for BIO8898 is largely hydrophobic and is lined by the side chains of residues L168, Y170, V228, E230, L259, and L261 of Chain A; Y170, Y172, A173, Q174, H224, and L225 of Chain B; and A123, H125, Y145, Y146, Y170, Y172, H224, S255, L259, and L261 of Chain C. The contact area between BIO8898 and the protein is 81% hydrophobic, 11% neutral, and 6% polar. The bipyridyl core of the inhibitor appears to π-stack with the Tyr172 side chain of subunit C, and the biphenyl group of Arm 4 makes a

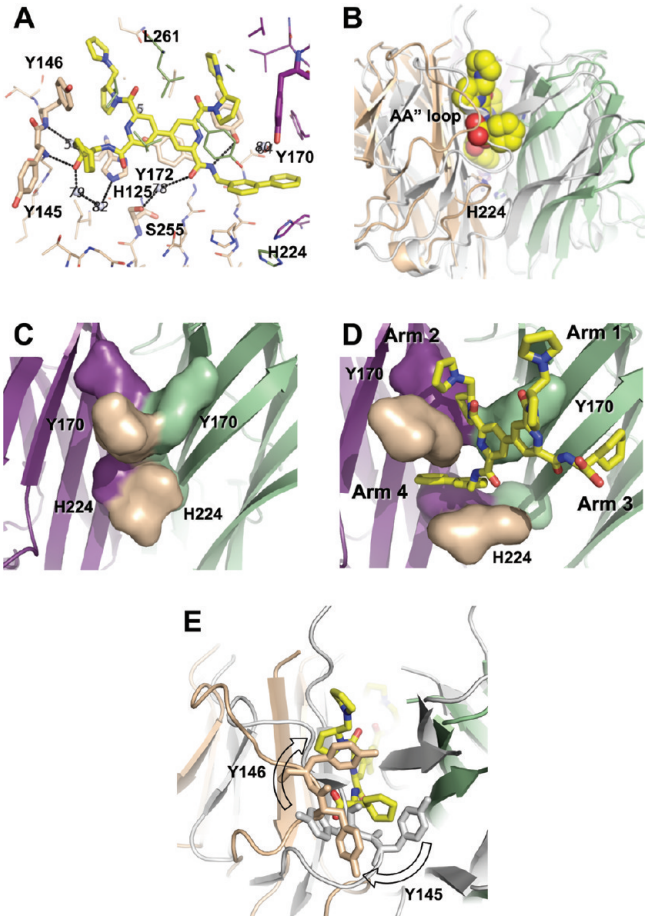

Figure 3. Details of the intermolecular interactions between BIO8898 and CD40L. (A) Hydrogen bonding interactions connecting protein, ligand, and ordered water molecules in the binding site. (B) Ribbons representation of the rigid-body conformational changes of CD40L bound to BIO8898 (colored by subunits) when superimposed with subunit B of unbound CD40L (gray). (C) Residues Y170 and H224 (shown in space-filling representation) contributed by each of the three CD40L subunits form a compact core in the native trimer. Subunit A has been removed from the representation, except for residues Y170 and H224 (shown in pale brown), to allow a clearer view of the core interactions. (D) Same view as in panel C but for the BIO8898/CD40L complex showing how Y170 and H224 conformationally adapt to accommodate the inhibitor. (E) The AA″ loop of subunit A undergoes a substantial conformational change from its position in the native trimer (shown in gray) to the position it occupies in the complex with BIO8898 (shown in pale brown) in which it covers the compound (yellow stick).

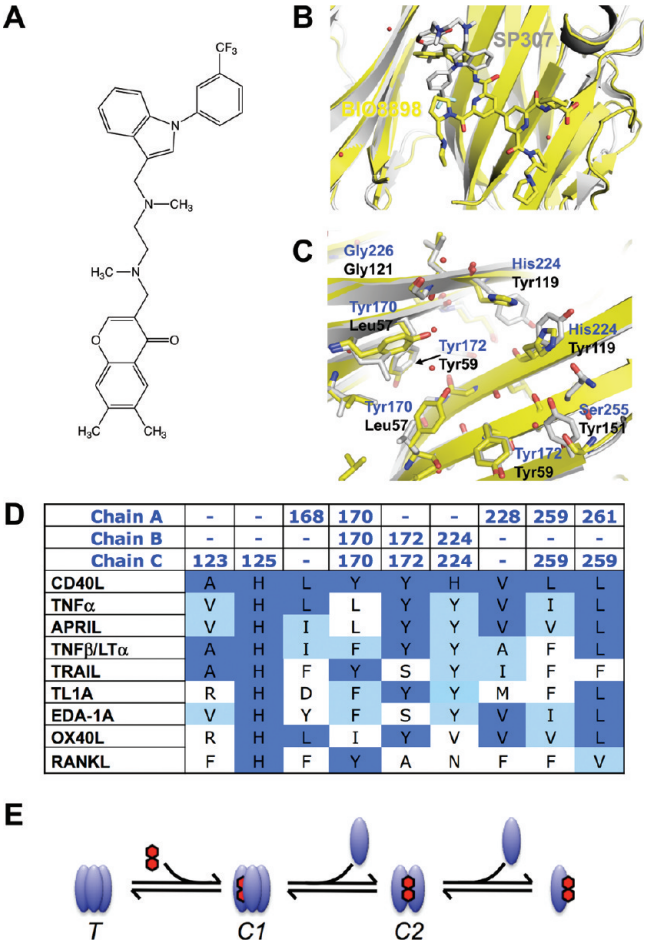

Chain A	-	-	168	170	-	-	228	259	261
Chain B	-	-	-	170	172	224	-	-	-
Chain C	123	125	-	170	172	224	-	259	259
CD40L	A	H	L	Y	Y	H	V	L	L
TNFα	V	H	L	L	Y	Y	V	I	L
APRIL	V	H	I	L	Y	Y	V	V	L
TNFβ/LTα	A	H	I	F	Y	Y	A	F	L
TRAIL	A	H	F	Y	S	Y	I	F	F
TL1A	R	H	D	F	Y	Y	M	F	L
EDA-1A	V	H	Y	F	S	Y	V	I	L
OX40L	R	H	L	I	Y	V	V	V	L
RANKL	F	H	F	Y	A	N	F	F	V

Figure 4. Comparison of BIO8898/CD40L complex to the SP307/TNFα complex reported in He *et al.*[12] (A) Structure of inhibitor SP307. (B) Superposition of backbone C-alphas of SP307/TNFalpha complex (gray) and the BIO8898/CD40L (yellow), with CD40L subunit A removed for clarity, illustrating that the SP307 and Arm 4 of BIO8898 bind in corresponding locations in the core of the protein. The N-termini of the protein are at the bottom of the figure and thus reversed from the orientation shown in Figure 3. (C) Similar side chains are involved in binding SP307 to TNFα (gray with black labels) and BIO8898 to CD40L (yellow with blue labels), including many conserved aromatic residues. (D) Structure-based sequence alignment of CD40L with other TNF-family members illustrating conservation in residues contacting BIO8898, in particular, residues 170, 172, and 224, which are exploited for BIO8898 interactions in more than 1 subunit and are highly homologous across several family TNF members. Color coding is as follows: dark blue, exact identity with CD40L; light blue, similar aromatic or hydrophobic side chains to those in CD40L. (E) Mechanism proposed by He *et al.*, for the inhibition of TNFα by SP307, in which *T* represents the intact trimeric cytokine and *C2* represents the complex of inhibitor with dimeric cytokine that was observed for TNFα with SP307. The species *C1* corresponds to a complex in which the inhibitor is intercalated into the protein trimer, as we report here for CD40L with BIO8898.

perpendicular $\pi-\pi$ interaction with Tyr172 from subunit B. While the compound is mainly bound by hydrophobic interactions, it also makes several hydrogen bonds (Figure 3A), all with subunit C. The inhibitor carboxylate group makes direct hydrogen bonds with the backbone amide of Tyr145 and water-mediated hydrogen bonds to the His125 and Tyr146 backbone amides, and the amide NH of the biphenyl arm donates a hydrogen bond to the phenol hydroxyl of Tyr170 while the amide carbonyl of this arm makes a water-mediated hydrogen bond to Ser255 (Figure 3A). These hydrogen bonds presumably help stabilize a specific orientation of the molecule within what is otherwise a highly nonpolar environment.

At least six water molecules can also be identified in the induced binding site in the complex (Figure 3A). These waters mediate protein−ligand binding and fill cavities that the inhibitor does not occupy. Two of these waters (nos. 79 and 56) are in good locations for their binding sites to be exploited by modification of the inhibitor, as they are hydrogen bonded to the carboxylate and may allow for easy library-based chemical modification to replace the carboxylate with larger, polar functional groups. Other waters (nos. 64, 51, and 80) occupy additional

dx.doi.org/10.1021/cb2000346 |*ACS Chem. Biol.* 2011, 6, 636–647

cavities in the binding site and particularly the central cavity. None of these buried water molecules are observed in the native CD40L trimer. Overall, the observed pharmacophore can be considered as one hydrogen bond donor and three acceptors on BIO8898 interacting with multiple hydrogen bond donors and acceptors on the protein, buried in an otherwise hydrophobic contact interface.

A phenomenon that has been invoked as an important feature of the binding of small molecule ligands to PPI targets is the ability of the protein to adapt its shape to better accommodate the organic ligand.[4,38] Comparing the structure of the bound CD40L molecule with that of the native protein provides insight into the extent to which structural adaptivity contributes to ligand binding in this system. While the largest structural changes are due to the translational split between the A and C subunits (Figures 2C and 3B), there are also conformational changes in both side chain and main chain atoms to accommodate specific portions of the inhibitor. In particular, residues His224 and Tyr170 from all three subunits, which in the native trimer come together to form a relatively close-packed core (Figure 3C), are displaced in the BIO8898-bound form (Figure 3D) such that the Tyr170 residues from chains A and C separate laterally to form a cleft that accommodates the proximal regions of Arms 2 and 4 and their connecting atoms. At the same time the three tyrosines separate axially from the three His224 side chains, which also rotate slightly, to form a deep lateral cavity that snugly accepts the projecting biphenyl group of Arm 4. Similarly, residues Leu259 from subunits A and C move apart to accommodate arm 2 of the inhibitor. Finally, the AA″ loop of subunit C, which includes Tyr145-Tyr146, reorganizes to form a flap that folds over Arms 1 and 3 of the inhibitor and partially shields them from solvent (Figure 3E). Thus, induction of the inhibitor binding site involves substantial local, intermediate range, and global changes in protein structure, of which the creation of a cleft between subunits A and C is just one part.

Mechanism of Inhibition. The mode of inhibition observed for BIO8898 can be compared to the recently reported inhibition of the homologous trimeric cytokine TNFα by the small molecule SP307 (Figure 4A).[12] Like BIO8898, SP307 disrupts the trimeric structure of a TNF family cytokine and binds to a newly exposed site in the core of the protein. However, SP307 disrupted the structure of the TNFα trimer to the extent that one protein subunit was fully ejected, leading to a complex in which the small molecule bound to the exposed core of an unprecedented dimeric form of the protein. Intriguingly, when the BIO8898/CD40L and SP307/TNFα complexes are superimposed, the binding site for SP307 in TNFα overlaps with the site in CD40L that accommodates Arm 4 of BIO8898 (Figure 4B). Moreover, in both cases inhibitor binding is dominated by interactions with aromatic residues on the protein. BIO8898/CD40L interacts with Y145 and Y146 (subunit C), Y170 (subunit A, B, and C), Y172 (subunits B, C), H224 (subunits B and C), and L261 (subunit A) (Figure 4C). In TNFα the binding site for SP307 is lined primarily by the side chains of six tyrosine residues, at positions 59, 115, and 119 on each of the two remaining protein subunits. Residues Leu57 and Tyr151 also make up part of the binding pocket (Figure 4C). For SP307 binding to dimeric TNFα the compound buries only a total of 98 Å^2 for this micromolar affinity interaction; the interface is composed of 74% nonpolar, 14% neutral, and 9% polar atoms, similar to the percentages observed for BIO8898 binding to CD40L but, unlike BIO8898, SP307 makes no hydrogen bonding interactions with the protein.

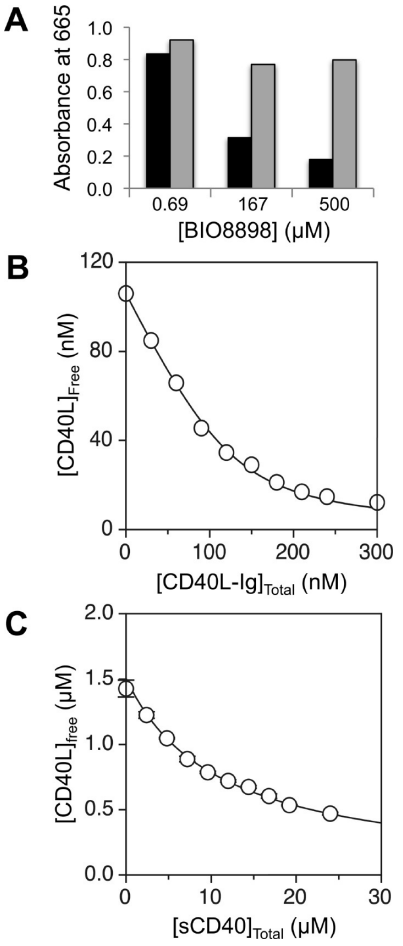

Figure 5. Dissociation and stoichiometry assays. (A) BIO8898 dose-dependently inhibits the binding of CD40-Ig to sparsely biotinylated CD40L that has been captured via a single biotin per trimer on a neutravidin-coated assay plate (black bars). However, if the assay plate is washed prior to CD40-Ig addition, to remove compound plus any dissociated CD40L subunits, no inhibition is observed (gray bars), showing that binding of BIO8898 does not cause irreversible disruption of CD40L or full ejection of CD40L subunits from the complex. The results shown are from a single experiment. (B) Binding of mycCD40L to CD40-Ig in solution, as measured using the initial rates Biacore titration method. Preincubation of individual samples each containing 100 nM CD40L with the indicated concentrations of CD40-Ig results in detection of lower concentrations of free CD40L, as the CD40L molecules that are bound by CD40-Ig in solution at equilibrium are blocked from binding to the CD40-Ig on the Biacore chip and thus are not detected. The solid line represents the best fit of the CD40L/CD40-Ig data to a quadratic binding equation, giving an apparent K_D for this interaction of 7.6 ± 2.1 nM (n = 13). (C) Similar experiment to that shown in panel B, except that samples containing fixed concentrations of 1.5 μM CD40L were preincubated with 0−24 μM monomeric sCD40 before each mixture was analyzed by Biacore. The data represent the mean of two Biacore measurements of each solution, separated by several hours. Error bars showing the spread of the duplicate data points are included but in most cases are smaller than the data symbol and cannot be seen. The solid line represents the best fit to a hyperbolic binding equation, indicating that CD40L binds monomeric sCD40 in solution only weakly, with K_D = 13 ± 2 μM (n = 2).

A preponderance of aromatic residues in the interface region is common to many TNF family cytokines (Figure 4D). The extensive similarities in both the binding locations and in the

types of interactions formed in the two complexes that have so far been observed suggest that this region of the core of TNF family trimers might represent a hot-spot for the binding of small molecules, potentially leading to conformational distortion or complete disruption of the trimeric ligand.

To test whether the inhibitory activity observed with BIO8898 results from formation of the one inhibitor per trimer complex seen crystallographically or, alternatively, whether in solution the binding of BIO8898 with CD40L causes ejection of one or more subunits as is the case with SP307 inhibition of TNFα, we directly tested the ability of BIO8898 to dissociate the CD40L trimer in solution using an assay analogous to that we used previously to characterize the dissociation of TNFα by SP307.[12] Briefly, singly biotinylated CD40L, captured on a neutravidin-coated assay plate, was incubated with compound at various concentrations. The ability of the captured CD40L to bind CD40-Ig was measured either with or without a prior wash step to remove any dissociated CD40L subunits. If trimer dissociation occurs, the dissociated subunits would be expected to recombine with each other in solution and then become lost upon washing, resulting in a loss of active CD40L from the assay plate. Figure 5A shows that incubation of the singly biotinylated CD40L with 167 or 500 μM compound inhibited CD40-Ig binding as expected, but if the plate was washed before CD40-Ig addition, then essentially no inhibition was observed. This result shows that inhibition by BIO8898 is reversible and does not cause dissociation of CD40L subunits. These results contrast with those from a similar assay with SP307 using singly biotinylated TNFα, in which this known trimer disruptor showed inhibition even when a wash step was included prior to addition of the soluble receptor, indicating that the compound caused dissociation of nonbiotinylated TNFα subunits from the assay plate.[12]

BIO8898 inhibits both receptor binding and functional activity of CD40L, indicating that formation of the BIO8898/CD40L complex renders the protein inactive. Of the three identical binding sites for CD40 that exist in native CD40L, only one is extensively disrupted in the BIO8898/CD40L complex. Intercalation of the inhibitor between CD40L subunits A and C pushes them apart by several angstroms, severely distorting the structure at that site. Moreover, portions of the inhibitor project into the solvent in a position that would likely occlude receptor binding. In addition, the inhibitor makes extensive interactions with the AA″ loop, which has been shown to be important for receptor binding.[18,39,40] The data in Figure 1B show that BIO8898 reduces the ability of CD40L to bind to CD40-Ig. To fully interpret how the structural distortion of CD40L in the complex with BIO8898 affects receptor binding, however, it is necessary to know whether the interaction of CD40L with CD40-Ig in our binding assay minimally requires occupancy of one, two, or three of the receptor binding sites on CD40L. If occupancy of only one or two binding sites per CD40L trimer is sufficient to achieve binding, then the inhibition observed in Figure 1B cannot be explained by disruption of just one of the trimer interfaces in the BIO8898/CD40L complex. Instead it would imply that the structural deformation of the CD40L trimer that occurs upon BIO8898 binding is sufficient to disrupt two or three of the receptor binding sites. To distinguish these possibilities, we characterized the binding of CD40L to CD40-Ig and also to a soluble monomeric form of CD40 extracellular domain (sCD40) by surface plasmon resonance (Biacore), using an initial rates ligand−receptor titration method that we have described previously.[41] Briefly, we incubated CD40L with CD40-Ig or sCD40 at several different molar ratios for sufficient time for binding to come to equilibrium. The equilibrium ratio of bound *versus* free CD40L at each molar ratio of CD40L with CD40-Ig or sCD40 was then measured by analyzing each equilibrated solution by Biacore, using the initial rate of CD40L binding to the CD40-Ig on the chip, under mass transport-limited conditions,[42] as a measure of free CD40L. This initial rates titration method has been shown previously to provide an accurate measure of the binding affinity and sometimes also the stoichiometry for the interaction of unlabeled proteins in solution.[41]

The results show that the binding of soluble CD40L to CD40-Ig in solution fits a single site binding model, giving an apparent binding affinity of 7.6 ± 2.1 nM ($n = 13$) (Figure 5B). In contrast, CD40L binds sCD40 approximately 1000-fold less strongly (K_D ~13 μM ($n = 2$)) (Figure 5C). To our knowledge this is the first quantitative measurement of the binding affinity of monomeric CD40 for a single binding site on CD40L but is fully consistent with previous reports that a bivalent or multivalent form of CD40 is required for strong binding to CD40L.[43−46] These results indicate that high affinity binding to CD40L requires cooperative binding of both CD40 "arms" of CD40-Ig to two adjacent binding sites on the CD40L trimer. The very weak binding observed for occupancy of a single CD40L binding site is insufficient to give a measurable signal under the conditions of the CD40L/CD40-Ig ELISA shown in Figure 1B, but occupancy of two binding sites by a single CD40-Ig molecule appears sufficient for strong binding. Therefore, the result that BIO8898 inhibits the binding of CD40L to CD40-Ig (Figure 1B) suggests that BIO8898 likely disrupts more than one receptor binding site on CD40L. Superposition of the complex structure with that of native CD40L by overlapping subunit B supports the existence of considerable distortion of the other two receptor binding sites (AB interface and BC interface), suggesting that the inhibitory effect of BIO8898 in part involves allosteric disruption of receptor binding sites adjacent to the site occupied by the compound (Supplementary Figure S3).

Comparison of the structural and inhibition data for BIO8898 with CD40L and SP307 with TNFα leads us to speculate that these two cases might represent variations on a common inhibition mechanism (Figure 4E). In both cases, the initial step is binding of the inhibitor to the trimeric cytokine to form a complex *C1* (Figure 4E) in which the native subunit interactions are significantly disrupted.[12] In the case of SP307 with TNFα this disruption was sufficient to cause ejection of a subunit, whereas for BIO8898 with CD40L the trimer remains intact but is structurally distorted to the extent that it can no longer bind strongly to CD40. In the case of SP307 with TNFα the initial 1:1 complex *C1* was not structurally characterized, but its existence was inferred from kinetic and biophysical data.[12] It is highly likely that the weakening of the intersubunit interactions in TNFα upon initial binding of SP307 are due to the intercalation of this inhibitor between two subunits, involving formation of an intermediate complex with an intercalated structure analogous to the stable complex observed for CD40L with BIO8898. The structure of BIO8898 with CD40L therefore potentially provides significant new insight into the first step of this trimer disruption mechanism. Moreover, a similar mechanism likely also accounts for the TNFα detrimerizing activity of the polyaromatic inhibitor Suramin[23] (Supplementary Figure S2) and for the recently reported inhibition of CD40L by Suramin[25] and other polyaromatic compounds,[26,27] though no structures of the inhibited complexes have yet been obtained in these cases. One difference between the binding modes of BIO8898 and SP307 is that in

addition to substantial hydrophobic contact BIO8898 also engages in several hydrogen bonds with the protein. Another important difference is that attempts to dock the missing third subunit of TNFα into the TNFα dimer/SP307 complex indicate that for SP307 to bind to a TNFα trimer in the observed location and conformation requires a much larger distortion of the protein trimer than is seen for CD40L with BIO8898. These differences in binding mode with BIO8898 presumably contribute to stabilization of the intercalated CD40L trimer compared to the protein dimer observed for SP307 with TNFα.

Lessons for Inhibition of PPI by Small Molecules. Our findings for inhibition of CD40L by BIO8898 corroborate several features that have been proposed as important for inhibition of PPI with small molecules. First, as has been observed in other systems,[47,48] a substantial degree of structural adaptivity at the binding site can be necessary to create a binding pocket for the inhibitor. Second, aromatic residues, and particularly tyrosines, appear to play a privileged role in protein-small molecule binding, especially at PPI interfaces.[49] Aromatic residues, as well as other amino acids such as Arg and Pro that possess planar or partly planar side chains, are known to be statistically over-represented at PPI interfaces[50−52] and are especially common at energetic hotspots for ligand−receptor binding. Tyrosines in particular are also highly over-represented at the antigen binding regions of antibodies.[53] It is noteworthy that BIO8898, SP307, Suramin, and several other molecules (Supplementary Figure S2) that are known or believed to inhibit TNF family proteins by trimer disruption all contain extensive polycyclic aromatic and/or biaryl functionality. The notion that aromatic groups are particularly favored in this regard is supported by a statistical analysis of the results of fragment-based screens against multiple targets, a substantial fraction of them protein−protein interactions, that identified biphenyls as a "privileged" structure for protein binding.[54]

If inhibiting transient PPI with small molecules is challenging, finding inhibitors against constitutive PPIs, which generally have more extensive interfaces and are higher in affinity,[9,10] might be considered an extreme form of this challenge. The results presented here suggest that this is not always the case, however. Constitutive PPI interfaces are considerably more hydrophobic than their transient counterparts, because the proteins involved do not need to be able to exist stably in monomeric form.[9,10] The activity of BIO8898 against CD40L and that of SP307 against TNFα suggest that in some cases this hydrophobicity, coupled with some structural adaptivity of interface residues, can translate into an ability to bind small molecules to form complexes of defined structure. Moreover, because only one of the three interactions in the constitutively trimeric CD40L need be disrupted to allow the inhibitor to bind, an exceptionally deep binding pocket can be created. This contrasts with the rather flat binding sites typically encountered when binding to one partner of a transient PPI. The mechanism observed for BIO8898 might be expected to apply to other constitutive complexes involving three or more protein subunits, potentially providing a means for these conventionally undruggable targets to form a binding site that possesses the characteristics, which are largely topological,[55] required to bind a drug with high affinity.

Three key questions define the potential utility of such an approach for drug discovery. Can molecules of this type be optimized to achieve the low nanomolar potency typically required of a drug? Can the ability of a small molecule to interact with such a site be made compatible with the requirement for acceptable pharmaceutical properties? Can such a molecule achieve adequate selectivity for the target site over hydrophobic sites in other proteins? Existing data do not provide definitive answers to any of these questions. However, with respect to the ability to inhibit TNF family members by trimer disruption the structure of BIO8898 with CD40L is encouraging, in that binding involves a combination of both hydrophobic and polar interactions, whereas the corresponding interactions between SP307 and TNFα were exclusively hydrophobic.[12] The BIO8898/CD40L structure therefore demonstrates that it is possible to target such a site with an inhibitor that presents a combination of polar and nonpolar interacting groups, providing increased prospects for selectivity and also for the level of solubility that is a prerequisite for good pharmaceutical properties.

METHODS

Expression and Purification of CD40L. A myc tagged form of soluble human CD40L was constructed with the amino acid sequence EQKLISEEDLNMGDQNPQIAAHVISEASSKTTSVLQWAEKGYYTMSNNLVTLENGKQLTVKRQGLYYIYAQVTFCSNREASSQAPFIASLCLKSPGRFERILLRAANTHSSAKPCGQQSIHLGGVFELQPGASVFVNVTDPSQVSHGTGFTSFGLLKL. The EQKLISEEDL peptide is the c-myc tag, the adjacent NM residues are an artifact of the cloning strategy, and the CD40L protein sequence begins with residue Gly116. The engineered DNA sequence was cloned into a derivative of the pPIC9 plasmid (Invitrogen) for expression in the yeast *Pichia pastoris* under control of the AOX1 promoter (methanol-inducible), fused to the PrePro alpha factor secretion signal of *Saccharomyces cerevisiae*. Plasmid DNA linearized with StuI in the HIS4 region of the plasmid was electroporated into GS115 *P. pastoris* following Invitrogen's instructions. Expression of CD40L protein in isolated clones was confirmed by SDS-PAGE and Western blotting with anti c-myc monoclonal antibody 9E10. Protein was expressed in Fernbach flasks using 1 L of BMGY medium for cell growth at 30 °C followed by 200 mL of BMMY (2% (v/v) methanol) medium for induction at 30 °C. Media recipes and growth protocols were according to Invitrogen standard *Pichia* protocols.

The expressed fusion protein was purified by anion exchange chromatography. The buffer exchanged supernatant (20 mM sodium phosphate pH 6.5) was passed through a Q Sepharose Fast Flow column (GE Healthcare), and the flow-through was loaded onto an SP sepharose column. After washing the column, the bound protein was eluted using 2X PBS (20 mM sodium phosphate dibasic, 3 mM potassium phosphate monobasic, 5 mM potassium chloride, 260 mM sodium chloride). The protein was >95% intact based on mass spectrometry. The protein was checked for purity by SDS-PAGE and was shown to be active by its ability to bind CD40-Ig as measured by Biacore.

Expression and Purification of CD40-Ig. A fusion of the CD40 extracellular domain and the human IgG1 Fc region was expressed using a DNA construct that was a kind gift from Ellen Garber (Biogen Idec) that encodes the amino acid sequence EAMEPPTACREKQYLINSQCCSLCQPGQKLVSDCTEFTETECLPCGESEFLDTWNRETHCHQHKYCDPNLGLRVQQKGTSETDTICTCEEGVKQIATGVSDTICEPCPVGFFSNVSSAFEKCHPWTSCETKDLVVQQAGTNKTDVVCGPQDRLRVDKTHTCPPCPAPELLGGPSVFLFPPKPKDTLMISRTPEVTCVVVDVSHEDPEVKFNWYVDGVEVHNAKTKPREEQYNSTYRVVSVLTKTKPREEQYNSTYRVVSVLTVLHQDWLNGKEYKCKVSNKALPAPIEKTISKAKGQPREPQVYTLPPSRDELTKNQVSLTCLVKGFYPSDIAVEWESNGQPENNYKTTPPVLDSDGSFFLYSKLTVDKSRWQQGNVFSCSVMHEALHNHYTQKSLSLSPGK. The CD40-Ig coding sequence was cloned and expressed in *P. pastoris* as described above for myc-CD40L, except that plasmid DNA was digested

with XbaI prior to electroporation and expression was verified with antihuman IgG1 serum.

CD40-Ig was expressed by fermentation using a modification of Invitrogen Basal Salts medium containing hexametaphosphate (R. Ohler, G. Lesnicki, and M. Galleno, personal communcation, Invitrogen Corp). This medium contained, per liter, 9 g ammonium sulfate, 0.93 g $CaSO_4$. $2H_2O$, 18.2 g $K_2SO_4.7H_20$, 14.9 g$MgSO_4.7H_2O$, 4.13 g KOH, 9 g NH_4SO_2, 20 g glycerol (all autoclaved), and 25 g sodium hexametaphosphate (Mallinckrodt) added after autoclaving. Ammonium hydroxide was used to maintain pH 6.0 during fermentation, with glycerol feeding to 100 g/L wet weight followed by feeding with a mixture of 75% (v/v) methanol + 25% (v/v) glycerol to induce protein production. The expressed fusion protein was captured by Protein-A affinity beads and further purified by anion exchange chromatography. Briefly, the cleared supernatant was dialyzed against PBS (10 mM sodium phosphate dibasic, 1.5 mM potassium phosphate monobasic, 2.5 mM potassium chloride, 130 mM sodium chloride). The buffer exchanged supernatant was then passed through a Protein-A Sepharose Fast Flow column (GE Healthcare), and the captured protein was eluted with a low pH buffer of 25 mM sodium phosphate pH 2.8. The peak fractions were pooled and dialyzed against 20 mM Tris-HCl pH 7.0, 50 mM NaCl. The dialyzed solution was loaded onto a Q Sepharose Fast Flow (GE Healthcare) column. After washing the column, the bound protein was eluted using a linear sodium chloride gradient from 50 to 500 mM. Mass spectrometric analysis of the protein indicated two major peaks comprising residues 1−404 and residues 3−404. The protein was checked for purity by SDS-PAGE and was shown to be active by its ability to bind mycCD40L as measured by Biacore.

Expression and Purification of sCD40. A soluble human CD40 extracellular domain was expressed using a DNA construct that was a kind gift of Ellen Garber (Biogen Idec) that encodes the amino acid sequence EAMEPPTACREKQYLINSQCCSLCQPGQKLVSDCTE-FTETECLPCGESEFLDTWNRETHCHQHKYCDPNLGLRVQQK-GTSETDTICTCEEGWHCTSEACESCVLHRSCSPGFGVKQIATG-VSDTICEPCPVGFFSNVSSAFEKCHPWTSCETKDLVVQQAGTN-KTDVVCG. The shCD40 coding sequence was cloned and expressed in *P. pastoris* as described above for CD40-Ig. The protein was purified from media by capturing on cation exchange chromatography and further purification by size exclusion chromatography. Briefly, the cleared supernatant was dialyzed against 25 mM sodium acetate pH4.0. The dialyzed solution was loaded onto a SP Sepharose Fast Flow (GE Healthcare) column. After washing the column, the bound protein was eluted with 20 mM sodium phosphate pH7.2 with 300 mM sodium chloride. The peak fractions were pooled and concentrated with Centricon concentrator (Millipore). The concentrated solution was then loaded onto a Superdex 75 Size Exclusion (GE Healthcare) column and eluted with PBS (10 mM sodium phosphate dibasic, 1.5 mM potassium phosphate monobasic, 2.5 mM potassium chloride, 130 mM sodium chloride). Mass spectrometric analysis of the protein indicated two major peaks comprising residues 1−170 and residues 3−170. The protein was monomeric as assessed by light scattering, displaying a single peak with apparent molecular weight of 22.7 kDa and was shown to be active by its ability to bind mycCD40L as measured by Biacore.

Synthesis of BIO8898. BIO8898 was prepared according to the method of Rebek and co-workers,[56] as described in WO2002018540 (A2,A3)[29] (Supplementary Figure 1). Details are as follows:

*(S)-N-(Biphenyl-3-ylmethyl)-4-bromo-6-(2-(pyrrolidin-1-ylmethyl)-pyrrolidine-1-carbonyl)-picolinamide (**2**).* 4-Bromo-2,6-pyridinedicarboxylic acid (**1**, 1.31 g, 5.33 mmol) was suspended in anhydrous dichloromethane (50 mL) and stirred at RT under nitrogen atmosphere as oxalyl chloride (1.92 mL, 21.9 mmol) was added dropwise and followed by one drop of dimethylformamide. The reaction mixture was stirred for 16 h, and the solvents were evaporated off. Toluene (10 mL) was added and evaporated off to give the acid chloride as a pale solid. The resulted acid chloride was then dissolved in anhydrous dichloromethane (32 mL) and added to a stirring solution of (*S*)-(+)-1-(2-pyrrolidinylmethyl)pyrrolidine (0.902 g, 5.86 mmol), 3-phenylbenzylamine (1.07 g, 5.86 mmol), and triethylamine (4.8 mL) in anhydrous dichloromethane (40 mL) at 0 °C under nitrogen. The reaction was allowed to warm to RT overnight. The reaction mixture was then concentrated by rotavap, and the residue was purified by flash column chromatography on silica to give the desired product as a white solid (0.91 g, 31% yield).

*(S)-tert-Butyl 2-(4-Bromo-6-((S)-2-(pyrrolidin-1-ylmethyl)pyrrolidine-1 carbonyl)picolinamido)-2-cyclohexylacetate (**3**).* Compound **3** (Supplementary Figure 1) was prepared in a similar manner to compound **2** but starting with 4-bromo-2,6-pyridinedicarboxylic acid, (*S*)-(+)-1-(2-pyrrolidinylmethyl)-pyrrolidine, and (*S*)-*tert*-butyl 2-amino-2-cyclohexylacetate.

*(S)-tert-Butyl 2-(2′-(Biphenyl-3-ylmethylcarbamoyl)-6,6′-bis((S)-2-(pyrrolidin-1-ylmethyl)-yrrolidine-1-carbonyl)-4,4′-bipyridine-2-carboxamido)-2cyclohexylacetate (**4**).* [1,1′-Bis(diphenylphosphino)ferrocene]dichloropalladium(II) (complex with CH_2Cl_2) (9 mg, 0.011 mmol) was added to a mixture of (*S*)-*N*-(biphenyl-3-ylmethyl)-4-bromo-6-(2-(pyrrolidin-1-ylmethyl)pyrrolidine-1-carbonyl)picolinamide (**2**) (200 mg, 0.366 mmol), bis(pinacolato)diboron (102 mg, 0.402 mmol), and potassium acetate (108 mg, 1.102 mmol) in anhydrous dimethylformamide (2.5 mL). The mixture was heated at 80 °C under nitrogen for 3 h. Additional portions of the palladium catalyst (9 mg) and bis(pinacolato)diboron (103 mg, 0.402 mmol) were added, and the mixture was heated until LC−MS showed the major formation of the desired product. The reaction was allowed to cool to RT, and the following were added: (*S*)-*tert*-butyl 2-(4-bromo-6-((S)-2-(pyrrolidin-1-ylmethyl)pyrrolidine-1-carbonyl)picolinamido)-2-cyclohexylacetate (**3**) (212 mg, 0.367 mmol), sodium carbonate (194 mg, 1.83 mmol), and water (1 mL). The resulting mixture was heated at 90 °C under nitrogen for 5 h. It was then cooled to RT and diluted with diethyl ether (10 mL) and water (10 mL). The aqueous layer was extracted with additional diethyl ether (10 mL). A small amount of precipitate was dissolved in dichloromethane and then combined with the diethyl ether extracts, which were then purified by a silica flash column (20 g) using dichloromethane/methanol/aqueous ammonia (99:1:0.1 to 93:7:0.7) as eluent.

(S)-2-(2′-(Biphenyl-3-ylmethylcarbamoyl)-6,6′-bis((S)-2-(pyrrolidin-1-ylmethyl)pyrrolidine-1-carbonyl)-4,4′-bipyridine-2-carboxamido)-2-cyclohexylacetic acid (BIO8898). (*S*)-*tert*-Butyl 2-(2′-(biphenyl-3-ylmethylcarbamoyl)-6,6′-bis((*S*)-2-(pyrrolidin-1-ylmethyl)-pyrrolidine-1-carbonyl)-4,4′-bipyridine-2-carboxamido)-2-cyclohexylacetate (**4**) (80 mg) was dissolved in dichloromethane (0.1 mL), and trifluoroacetic acid (0.9 mL) was added. The reaction was stirred at RT overnight. The solvents were evaporated off, and trituration with diethyl ether (10 mL) gave an off-white solid that was further purified by HPLC with 5−95% 0.1%TFA/acetonitrile and water to give the desired product as a white solid. MS/MH+: 910.32 and 455.57; ^{1}H NMR (300 MHz, DMSO-d_6) δ ppm 0.96−1.32 (m, 6 H) 1.69−1.80 (m, 6 H) 1.78−2.22 (m, 14 H) 2.54 (s, 1 H) 3.18 (br. s., 3 H) 3.27−3.43 (m, 2 H) 3.44−3.61 (m, 2 H) 3.63−3.93 (m, 6 H) 4.0−4.64 (m, 8 H) 4.67 (d, J = 6.41 Hz, 2 H) 7.36 (dd, J = 7.16, 5.30 Hz, 1 H) 7.45 (dd, J = 15.45, 7.80 Hz, 2 H) 7.56 (d, J = 7.2 Hz, 1 H) 7.62 (d J = 7.62, 2 H) 7.71 (d J = 15.1, 1 H) 8.39 (d, J = 1.13 Hz, 1 H) 8.42−8.50 (m, 2 H) 8.50−8.57 (m, 1 H) 8.54 (dd, J = 5.27, 1.5 Hz, 1 H) 8.60−8.78 (m, 1 H) 9.30 (t, J = 6.03 Hz, 1 H) 9.54−9.60 (m, 1 H) 9.78−9.97 (m, 1 H).

Crystallization and Structure Determination. BIO8898 was incubated at RT for 1 h with 8 mg mL^{-1} CD40L trimer at 1 mM concentrations in the presence of 2% (v/v) DMSO. Needle-like crystals of CD40L complexed to BIO8898 (Table 1) were initially identified in hanging drop vapor diffusion setups under a 1:1 volume ratio of complex and a crystallization condition consisting of 24% (v/v) Peg3350, 50 mM Hepes pH 7.5, 0.2 M sodium citrate at 20 °C. In optimization efforts, the best plate-like crystals appeared from hanging drops using a 1:1 ratio of

Table 1. X-ray Data Collection and Refinement Statistics

property	value
space group	$P2_12_12_1$
cell dimensions	
a, *b*, *c* (Å)	63.3,67.6, 108.5
α, *β*, *γ* (deg)	90.0, 90.0, 90.0
resolution (Å)	50−2.5 (2.59−2.50)[a]
R_{merge}	0.050 (0.157)
$I/\sigma I$	30.7 (5.8)
completeness (%)	98.5 (92.5)
redundancy	3.98 (3.20)
refinement	
resolution (Å)	20−2.5
no. reflections	15,594
R_{work}/R_{free}	22.6 (29.8)
no. atoms	
protein	2997
ligand	67
sugars	117
water	73
B-factors (Å^2)	
Wilson B	58.4
protein	37.1
ligand	32.8
sugars	67.8
water	40.9
rms deviations	
bond lengths (Å)	0.017
bond angles (deg)	1.91

[a] Data collected on single crystal. Highest resolution shell is shown in parentheses.

protein to a crystallization condition consisting of 25% Peg 3350, 0.1 M sodium cacodylate pH 6.5, 0.2 M ammonium acetate, and 5% (v/v) glycerol. No crystals were observed in parallel drops without BIO8898. The fragile crystals were frozen directly from mother liquor into liquid nitrogen.

Native data was collected from a single crystal frozen at −180 °C at beamline X25 at the National Synchrotron Light Source (Upton, NY) with X-rays at a 1.1 Å wavelength (Table 1). Data processing to 2.5 Å was carried out with the HKL data package version 1.97.2.[57] The crystals belong to space group $P2_12_12_1$ with unit cell dimensions a = 63.3 Å, b = 67.6 Å, c = 108.5 Å, $\alpha = \beta = \gamma = 90°$, which are consistent with a single CD40L trimer per asymmetric unit (Table 1). The structure was solved by molecular replacement with the program AMORE [58] using the CD40L trimer as a search model and using a subset of data to 3.0 Å resolution. The resultant R_{free} was 55% and correlation coefficient was 29.2. By using a 3-body rigid-body refinement protocol in CNX,[59] in which each of the three monomers of the CD40L trimer were treated as a rigid body, the R_{free} dropped to 47% using the subset of data to 3.0 Å. An Fo-Fc difference map showed clear density for a small molecule in the center of the trimer. Refinement was carried out in CNX using an mlf target and reserving 5% of the reflections for the test set to 2.5 Å native data and was further refined in Refmac5.[60] The final model has an R-factor of 22.6% and an R_{free} of 29.8% and consists of residues 122−178, 183−261 (chain A), 121−131, 135−180, 187−261 (chain B), 121−261 (chain C), one BIO8898, 3 glycan chains, and 77 waters. Ramachandran plots [61] indicate that 0% of the model is in disallowed regions and 0% in generously allowed regions.

CD40L/CD40-Ig Dissociation Enhanced Lanthanide Fluorescence Immunoassay (DELFIA). Microtiter plates (Nunc Maxisorp) were coated overnight with 100 μL CD40-Ig at 5 μg mL^{-1} in PBS, pH 7.2 at 4 °C, washed three times with PBS containing 0.05% (v/v) Tween (PBS-T), and blocked for 1 h with Superblock in PBS (200 μL, Pierce) at RT. Compounds were serially diluted 3-fold in DMSO (0.025−500 μM) added to the plate along with 0.04 μg mL^{-1} myc-CD40L in assay buffer (2% (v/v) Superblock, PBS, pH 7.4, final volume 100 μL). The reaction contained 1% DMSO final and was incubated for 1 h at RT, washed three times with PBS-T, and binding was detected by the addition of 100 μL of a 29 μg mL^{-1} solution of Europium-Antimyc (Perkin-Elmer) in DELFIA assay buffer (Perkin-Elmer) for 1 h at RT. The wells were washed 8 times with PBS-T, 100 μL of DELFIA enhancement solution (Perkin-Elmer) was added, and the plate was mixed for 5 min at RT. Time-resolved fluorimetry measurements were made using an Analyst plate reader (Molecular Devices), and the percent activity at a given compound concentration was calculated using the following equation: % activity =100(signal with compound/signal without compound) which was used to generate IC_{50} curves. The data was generated in triplicate and averaged with error bars shown. Data were fitted to a hyperbolic inhibition equation with a nonzero offset: Activity = $A_{max}-\{(A_{max}\text{-}A_{min})[BIO8898]/(IC_{50}+[BIO8898])\}$, where A_{max} and A_{min} represents maximum and minimum % activity (*i.e.*, activity at zero [BIO8898] and saturating [BIO8898], respectively), and IC_{50} represents the concentration of BIO8898 giving 50% inhibition (*i.e.*, giving % A = $(A_{max}\text{-}A_{min})/2 + A_{min}$).

CD40L-Mediated Apoptosis Assay. MTT (3-[4,5-Dimethylthiazol-2-yl]-2,5-diphenyl-teteazolium bromide) (Sigma M-2128) and cyclohexamide (CHX; Sigma, C-7698) were purchased from Sigma-Aldrich Corp. Baby hamster kidney (BHK) cells, stably transfected with a chimeric receptor containing the extracellular domain of human CD40 and the intracellular domain of human TNFR1 (CD40-TNFR-BHK), were kindly provided by Dr. Hartmut Engelmann, University of Munich, Germany, and were grown in RPMI medium containing 10% (v/v) heat-inhibited fetal bovine serum, 2 mM L-Glutamine, 50 U ml^{-1} Penicillin/Streptomycin, and 600 μg mL^{-1} G418.

CD40-TNFR-BHK cells were cultured with a density of 5 × 10^4 cells per well in 96-well plate. A stock solution of BIO8898 in DMSO was serially diluted in culture medium, premixed with soluble CD40L and CHX to final concentrations of 3 ng mL^{-1} and 50 μg mL^{-1}, respectively, and added to the cultures in 96-well plates. On the third day, 10 μL of MTT (5 mg mL^{-1} in PBS) was added to each well, and the plates were incubated for 4 h, followed by addition of 100 μL 10% SDS/0.01 N HCl, and a further incubation overnight at 37 °C. The number of viable cells in each well was assessed by measuring the optical absorbance at 590 nm for each well. Data were fitted using a hyperbolic equation: $A_{590} = A_{590}(min) + \{(A_{590}(max) - A_{590}(min))([BIO8898]/EC_{50} + [BIO8898])\}$, where $A_{590}(max)$ and $A_{590}(min)$ represent the minimum and maximum absorbance values, and EC_{50} represents the concentration of BIO8898 that gave an A_{590} value halfway between $A_{590}(min)$ and the extrapolated value for $A_{590}(max)$. The data in Figure 1C do not approach saturation because the maximum concentration of BIO8898 that could be used in the assay was limited by its low solubility and the low tolerance of the assay for DMSO. Nevertheless, data were obtained up to a concentration of BIO8898 of 111 μM, which exceeds the fitted EC_{50} value of ~69 μM, suggesting that this value reflects a valid if approximate estimate of the potency of BIO8898 in this assay.

CD40L Trimer Disruption Assay. The ability of BIO8898 to cause the dissociation of the CD40L trimer was measured using an assay analogous to that established for the TNFα trimer disruptor SP307.[12] Briefly, sparsely biotinylated CD40L designed to possess no more than one biotin molecule per trimer was prepared by reacting 10 mol equiv of CD40L Q186C mutant (calculated based on the monomer) with 1 equiv of Sulfo-NHS-LC-biotin (Pierce) in 50 mM sodium carbonate, pH 9.0

with 150 mM NaCl for 60 min at RT. The reaction was quenched with 10 mM ethanolamine and purified by gel filtration. The singly biotinylated CD40L was captured on neutravidin-coated assay plates and then incubated with BIO8898 at various concentrations or with assay buffer alone containing 1% (v/v) DMSO. The ability of the captured CD40L to bind CD40-Ig was measured either with or without a prior wash step to remove any dissociated CD40L subunits. If trimer dissociation occurs the dissociated subunits would be expected to recombine with each other in solution and then become lost upon washing, resulting in a loss of active CD40L from the assay plate and a reduction in the binding of CD40-Ig. The data shown are the results of a single experiment.

Biacore Binding Measurements. All experiments were performed using a Biacore 3000 instrument (GE Healthcare).

Biacore Chip Surface Preparation. CD40-Ig was immobilized on CM5 sensorchips (GE Healthcare) using the Biacore Amine Coupling Kit according to the manufacturer's instructions. Briefly, CD40-Ig was diluted to 50 μg mL^{-1} in 10 mM acetate, pH 5.0, and 50 μL was injected over chip surfaces that had been activated with a 50 μL injection of 1:1 *N*-hydroxysuccinimide (NHS)/1-ethyl-3(3-dimethylaminopropyl)-carbodiimide hydrochloride (EDC). Remaining activated carboxylate esters on the chip surface were capped by injecting 50 μL of 1 M ethanolamine over the chip surface. Typical immobilization levels were 4000−6000 RU.

Solution-Phase Biacore Binding Assays. The binding of soluble CD40L to CD40-Ig or sCD40 was measured in solution using the initial rates receptor−ligand Biacore titration method we have described previously.[41] Briefly, CD40L was mixed in various molar ratios with CD40-Ig or sCD40 in HBS buffer (10 mM HEPES pH 7.0, 150 mM NaCl, 3.4 mM EDTA, 0.05% P-20 detergent plus 0.05% BSA) and incubated at 4 °C for a minimum time of 3 h. This same buffer was used as the running buffer during sample analysis, and 50 μL of each pre-equilibrated solution was then injected at 5 μL min^{-1} over a CD40-Ig derivatized surface, or over an adjacent, underivatized surface as a background control, followed by a 3 min dissociation in HBS buffer. Following each reaction cycle the Biacore chip surface was regenerated with 2 × 20 μL injections of 2 M Guanidine-HCL + 0.5 M KCl. Under these experimental conditions the binding is mass transport limited during approximately the first minute of binding. The mass transport limited region of the sensorgrams was determined from the region where the slope of a first derivative plot of dRU/d*t* was zero. During the mass transport limited binding phase the initial rate of binding (V_i) is proportional to the concentration of free ligand in solution.[42] As only free CD40L is able to bind to the CD40-Ig surface, V_i therefore acts as a measure of the concentration of free CD40L in each solution.[41] A plot of the initial rate of binding (Vi) measured at various concentrations of CD40L alone was fitted to a straight line to give a standard curve that was used to convert V_i values to $[\mathrm{CD40L}]_{\mathrm{free}}$ values for subsequent measurements. The binding affinity was determined by plotting $[\mathrm{CD40L}]_{\mathrm{free}}$ *versus* $[\mathrm{CD40\text{-}Ig}]_{\mathrm{total}}$ and fitting the data to the following quadratic binding equation:

$$[\mathrm{L}]_{\mathrm{f}} = \left[[\mathrm{L}]_{\mathrm{T}} - \frac{1}{2}\{(n[\mathrm{R}]_{\mathrm{T}} + [\mathrm{L}]_{\mathrm{T}} + K_{\mathrm{D}}) - \sqrt{(n[\mathrm{R}]_{\mathrm{T}} + [\mathrm{L}]_{\mathrm{T}} + K_{\mathrm{D}})^2 - 4n[\mathrm{R}]_{\mathrm{T}}[\mathrm{L}]_{\mathrm{T}}}\}\right]$$

where $[\mathrm{L}]_{\mathrm{f}}$ (*i.e.*, the *y* axis variable) equals the concentration of free CD40L present in a given solution; $[\mathrm{L}]_{\mathrm{T}}$ is the total CD40L concentration present in each sample; $[\mathrm{R}]_{\mathrm{T}}$ is the total CD40-Ig concentration present in the solutions; *n* is the stoichiometry of CD40-Ig binding to CD40L; and K_{D} is the binding affinity. The affinity of the monomeric sCD40 binding to CD40L was determined using the same method by preincubating a fixed concentration of CD40L with various concentrations of sCD40, determining $[\mathrm{CD40L}]_{\mathrm{free}}$ for each sample at equilibrium as described above, and then plotting $[\mathrm{CD40L}]_{\mathrm{free}}$ *versus* $[\mathrm{sCD40}]_{\mathrm{total}}$ and fitting the data to hyperbolic binding equation: $[\mathrm{L}]_{\mathrm{f}} = [\mathrm{L}]_{\mathrm{T}} - [\mathrm{L}]_{\mathrm{T}}\{[\mathrm{R}]_{\mathrm{T}}/(K_{\mathrm{D}} + [\mathrm{R}]_{\mathrm{T}})\}$, where $[\mathrm{L}]_{\mathrm{f}}$, $[\mathrm{L}]_{\mathrm{T}}$, $[\mathrm{R}]_{\mathrm{T}}$ and K_{D} have the definitions given above. The interaction was sufficiently weak that no stoichiometry information is contained in the data. A hyperbolic curve fit was appropriate for the weak binding of sCD40 because the experiment was performed under conditions where the concentration of the fixed component, CD40L, was low compared to K_{D}; for the experiment with CD40-Ig the fixed component was present at a concentration that was high compared to K_{D}, necessitating the use of a quadratic binding equation.[41]

■ ASSOCIATED CONTENT

Supporting Information. This material is available free of charge *via* the Internet at http://pubs.acs.org.

Accession Codes

The structure has been deposited with PDB code 3LKJ.

■ AUTHOR INFORMATION

Corresponding Author

*E-mail: whitty@bu.edu; laura.silvian@biogenidec.com.

Present Addresses

[⊥]Vertex Pharmaceuticals Inc., 130 Waverly St., Cambridge, MA 02139.

[∥]Roche Pharmaceuticals, Palo Alto, CA 94304.

[#]WinerGen Technologies Inc., Ltd., Biotech Center, Gaoxin district, Weifang, PR China.

Notes

The authors with the exception of B.C. and A.F. are at present or were at one time Biogen Idec employees and owned or still own Biogen Idec stock.

■ ACKNOWLEDGMENT

The authors would like to acknowledge P.A. Boriack-Sjodin for aid in data collection and A. Saxena for access to X25 beamtime at the NSLS. This work was supported in part by NIH grant 1R01GM094551 to A.W.

■ REFERENCES

(1) Wells, J. A., and McClendon, C. L. (2007) Reaching for high-hanging fruit in drug discovery at protein−protein interfaces. *Nature 450*, 1001–1009.

(2) Gerrard, J. A., Hutton, C. A., and Perugini, M. A. (2007) Inhibiting protein-protein interactions as an emerging paradigm for drug discovery. *Mini-Rev. Med. Chem. 7*, 151–157.

(3) Fischer, P. (2005) Protein-protein interactions in drug discovery. *Drug Des. Rev. Online 2*, 179–207.

(4) Whitty, A., and Kumaravel, G. (2006) Between a rock and a hard place? *Nat. Chem. Biol. 2*, 112–118.

(5) Ganesan, A. (2008) The impact of natural products upon modern drug discovery. *Curr. Opin. Chem. Biol. 12*, 306–317.

(6) Vu, B. T., and Vassilev, L. T. (2010) Small-molecule inhibitors of the p53-MDM2 interaction. *Curr. Top. Microbiol. Immunol. 348*, 151–172.

(7) Dynek, J. N. and Vucic, D. (2010) Antagonists of IAP proteins as cancer therapeutics. *Cancer Lett.* Epub ahead of print; DOI: 10.1016/j.canlet.2010.06.013.

(8) Wilson, W. H., O'Connor, O. A., Czuczman, M. S., LaCasce, A. S., Gerecitano, J. F., Leonard, J. P., Tulpule, A., Dunleavy, K., Xiong, H., Chiu, Y. L., Cui, Y., Busman, T., Elmore, S. W., Rosenberg, S. H., Krivoshik, A. P., Enschede, S. H., and Humerickhouse, R. A. (2010) Navitoclax, a targeted high-affinity inhibitor of BCL-2, in lymphoid

malignancies: a phase 1 dose-escalation study of safety, pharmacokinetics, pharmacodynamics, and antitumour activity. *Lancet Oncol. 11*, 1149–1159.

(9) Headd, J. J., Ban, Y. E., Brown, P., Edelsbrunner, H., Vaidya, M., and Rudolph, J. (2007) Protein-protein interfaces: properties, preferences, and projections. *J. Proteome Res. 6*, 2576–2586.

(10) Nooren, I. M., and Thornton, J. M. (2003) Structural characterisation and functional significance of transient protein-protein interactions. *J. Mol. Biol. 325*, 991–1018.

(11) Bannwarth, L., and Reboud-Ravax, M. (2007) An alternative strategy for inhibiting multidrug-resistant mutants of the dimeric HIV-1 protease by targeting the subunit interface. *Biochem. Soc. Trans. 35*, 551–554.

(12) He, M. M., Smith, A. S., Oslob, J. D., Flanagan, W. M., Braisted, A. C., Whitty, A., Cancilla, M. T., Wang, J., Lugovskoy, A. A., Yoburn, J. C., Fung, A. D., Farrington, G., Eldredge, J. K., Day, E. S., Cruz, L. A., Cachero, T. G., Miller, S. K., Friedman, J. E., Choong, I. C., and Cunningham, B. C. (2005) Small-molecule inhibition of TNF-alpha. *Science 310*, 1022–1025.

(13) Schonbeck, U., and Libby, P. (2001) The CD40/CD154 receptor/ligand dyad. *Cell. Mol. Life Sci. 58*, 4–43.

(14) Daikh, D. I., Finck, B. K., Linsley, P. S., Hollenbough, D., and Wofsy, D. (1997) Long-term inhibition of murine lupus by brief simultaneous blockade of the B7/CD28 and CD40/gp39 costimulation pathways. *J. Immunol. 159*, 3104–3108.

(15) Cho, C. S., Burkly, L. C., Fechner, J. H., Jr., Kirk, A. D., Oberley, T. D., Dong, Y., Brunner, K. G., Peters, D., Tenhoor, C. N., Nadeou, K., Yagci, G., Ishido, N., Schultz, J. M., Tsuchida, M., Hamawy, M. M., and Knechtle, S. J. (2001) Successful conversion from conventional immunosuppression to anti-CD40L monoclonal antibody costimulatory molecule blockade in rhesus renal allograft recipients. *Transplantation 72*, 587–597.

(16) Sho, M., Sandner, S. E., Najafian, N., Salama, A. D., Dong, V., Yamada, A., Kishimoto, K., Haraa, H., Schmitt, I., and Sayegh, M. H. (2002) New insights into the interactions between T-cell costimulatory blockade and conventional immunosuppressive drugs. *Ann. Surg. 236*, 667–675.

(17) Schonbeck, U., and Libby, P. (2001) CD40 signaling and plaque instability. *Circ. Res. 89*, 1092–1103.

(18) Karpusas, M., Lucci, J., Ferrant, J., Benjamin, C., Taylor, F. R., Strauch, K., Garber, E., and Hsu, Y. M. (2001) Structure of CD40 ligand in complex with the Fab fragment of a neutralizing humanized antibody. *Structure 9*, 321–329.

(19) Singh J, G. E., Van Vlijmen, H, Karpusas, M, Hsu, Y. M., Zheng, Z, Naismith, J. H., and Thomas, D. (1998) The role of polar interactions in the molecular recognition of CD40L with its receptor CD40. *Protein Sci. 7*, 1124–1135.

(20) Boumpas, D. T., Furie, R., Manzi, S., Illei, G. G., Wallace, D. J., Balow, J. E, and Vaishnaw, A. (2003) A short course of BG9588 (anti-CD40 ligand antibody) improves serologic activity and decreases hematuria in patients with proliferative lupus glomerulonephritis. *Arthritis Rheum. 48*, 719–727.

(21) Ferrant, J. L., Benjamin, C. D., Cutler, A. H., Kalled, S. L., Hsu, Y.-M., Garber, E. A., Hess, D. M., Shapiro, R. I., Kenyon, N. S., Harlan, D. M., Kirk, A. D., Burkly, L. C., and Taylor, F. R. (2004) The contribution of Fc effector mechanisms in the efficacy of anti-CD154 immunotherapy depends on the nature of the immune challenge. *Int. Immunol. 16*, 1583–1594.

(22) Voogd, T. E., Vansterkenburg, E. L., Wilting, J., and Janssen, L. H. (1993) Recent research on the biological activity of suramin. *Pharmacol. Rev. 45*, 177–203.

(23) Alzani, R., Corti, A., Grazioli, L., Cozzi, E., Ghezzi, P., and Marcucci, F. (1993) Suramin induces deoligomerization of human tumor necrosis factor alpha. *J. Biol. Chem. 268*, 12526–12529.

(24) Grazioli, L., Alzani, R., Ciomei, M., Mariani, M., Restivo, A., Cozzi, E., and Marcucci, F. (1992) Inhibitory effect of suramin on receptor binding and cytotoxic activity of tumor necrosis factor alpha. *Int. J. Immunopharmacol. 14*, 637–642.

(25) Margolles-Clark, E., Jacques-Silva, M. C., Ganesan, L., Umland, O., Kenyon, N. S., Ricordi, C., Berggren, P. O., and Buchwald, P. (2009) Suramin inhibits the CD40-CD154 costimulatory interaction: a possible mechanism for immunosuppressive effects. *Biochem. Pharmacol. 77*, 1236–1245.

(26) Margolles-Clark, E., Umland, O., Kenyon, N. S., Ricordi, C., and Buchwald, P. (2009) Small-molecule costimulatory blockade: organic dye inhibitors of the CD40-CD154 interaction. *J. Mol. Med. 87*, 1133–1143.

(27) Margolles-Clark, E., Kenyon, N. S., Ricordi, C., and Buchwald, P. (2010) Effective and specific inhibition of the CD40-CD154 costimulatory interaction by a naphthalenesulphonic acid derivative. *Chem. Biol. Drug Des. 76*, 305–313.

(28) Ganesan, L., Margolles-Clark, E., Song, Y., and Buchwald, P. (2011) The food colorant erythrosine is a promiscuous protein-protein interaction inhibitor. *Biochem. Pharmacol. 81*, 810–818.

(29) Zheng, Z., Carter, M.-B., Liao, Y., Sun, L., Kirkovsky, L., Mrose, S., Hsu, Y., Thomas, D., Shipps, G. W., Jr., Jindal, S., Lenz, G. R., and Nash, H. M. (2002) Novel CD40:CD154 binding interruptor compounds and use thereof to treat immunological complications, (WIPO, Ed.) C12N ed., Biogen, Inc.

(30) Annis, D. A., Nazef, N., Chuang, C. C., Scott, M. P., and Nash, H. M. (2004) A general technique to rank protein-ligand binding affinities and determine allosteric versus direct binding site competition in compound mixtures. *J. Am. Chem. Soc. 126*, 15495–15503.

(31) Jurgens, G., Hermann, A., Aktuna, D., and Petek, W. (1992) Dissociation-enhanced lanthanide fluorescence immunoassay of lipoprotein(a) in serum. *Clin. Chem. 38*, 853–859.

(32) Schwabe, R. F., Hess, S., Johnson, J. P., and Engelmann, H. (1997) Modulation of soluble CD40 ligand bioactivity with anti-CD40 antibodies. *Hybridoma 16*, 217–226.

(33) Plumb, J. A. (2004) Cell sensitivity assays: the MTT assay. *Methods Mol. Med. 88*, 165–169.

(34) Coan, K. E., and Shoichet, B. K. (2008) Stoichiometry and physical chemistry of promiscuous aggregate-based inhibitors. *J. Am. Chem. Soc. 130*, 9606–9612.

(35) Feng, B. Y., Simeonov, A., Jadhav, A., Babaoglu, K., Inglese, J., Shoichet, B. K., and Austin, C. P. (2007) A high-throughput screen for aggregation-based inhibition in a large compound library. *J. Med. Chem. 50*, 2385–2390.

(36) Karpusas, M., Hsu, Y. M., Wang, J. H., Thompson, J., Lederman, S., Chess, L., and Thomas, D. (1995) 2 A crystal structure of an extracellular fragment of human CD40 ligand. *Structure 3*, 1426.

(37) Reynolds, C., Damerell, D., and Jones, S. (2009) ProtorP: a protein-protein interaction analysis server. *Bioinformatics 25*, 413–414.

(38) Braisted, A. C., Oslob, J. D., Delano, W. L., Hyde, J., McDowell, R. S., Waal, N., Yu, C., Arkin, M. R., and Raimundo, B. C. (2003) Discovery of a potent small molecule IL-2 inhibitor through fragment assembly. *J. Am. Chem. Soc. 125*, 3714–3715.

(39) Fournel, S., Wieckowski, S., Sun, W., Trouche, N., Dumortier, H., Bianco, A., Chaloin, O., Habib, M., Peter, J. C., Schneider, P., Vray, B., Toes, R. E., Offringa, R., Melief, C. J., Hoebeke, J., and Guichard, G. (2005) C3-symmetric peptide scaffolds are functional mimetics of trimeric CD40L. *Nat. Chem. Biol. 1*, 377–382.

(40) Bajorath, J., Chalupny, N. J., Marken, J. S., Siadak, A. W., Skonier, J., Gordon, M., Hollenbaugh, D., Noelle, R. J., Ochs, H. D., and Aruffo, A. (1995) Identification of residues on CD40 and its ligand which are critical for the receptor-ligand interaction. *Biochemistry 34*, 1833–1844.

(41) Day, E. S., Cachero, T. G., Qian, F., Sun, Y., Wen, D., Pelletier, M., Hsu, Y. M., and Whitty, A. (2005) Selectivity of BAFF/BLyS and APRIL for binding to the TNF family receptors BAFFR/BR3 and BCMA. *Biochemistry 44*, 1919–1931.

(42) (1998) *BIAtechnology Handbook*, p 6-5, Biacore AB.

(43) Holler, N., Kataoka, T., Bodmer, J. L., Romero, P., Romero, J., Deperthes, D., Engel, J., Tschopp, J., and Schneider, P. (2000) Development of improved soluble inhibitors of FasL and CD40L based on oligomerized receptors. *J. Immunol. Methods 237*, 159–173.

(44) He, X. H., Xu, L. H., and Liu, Y. (2006) Enhancement of binding activity of soluble human CD40 to CD40 ligand through incorporation of an isoleucine zipper motif. *Acta Pharmacol. Sin. 27*, 333–338.
(45) Van Broekhoven, C. L., and Altin, J. G. (2001) A novel system for convenient detection of low-affinity receptor-ligand interactions: chelator-lipid liposomes engrafted with recombinant CD4 bind to cells expressing MHC class II. *Immunol. Cell Biol. 79*, 274–284.
(46) Hollenbaugh, D., Douthwright, J., McDonald, V., and Aruffo, A. (1995) Cleavable CD40Ig fusion proteins and the binding to sgp39. *J Immunol. Methods 188*, 1–7.
(47) Brown, S. P., and Hajduk, P. J. (2006) Effects of conformational dynamics on predicted protein druggability. *ChemMedChem 1*, 70–72.
(48) Arkin, M. R., Randal, M., DeLano, W. L., Hyde, J., Luong, T. N., Oslob, J. D., Raphael, D. R., Taylor, L., Wang, J., McDowell, R. S., Wells, J. A., and Braisted, A. C. (2003) Binding of small molecules to an adaptive protein-protein interface. *Proc. Natl. Acad. Sci. U.S.A. 100*, 1603–1608.
(49) Whitty, A. (2008) Small-molecule inhibitors of protein-protein interactions: challenges and prospects, in *Gene Family Targeted Molecular Design* (Lackey, K. E., Ed.), pp 199−226, Wiley, Hoboken.
(50) Bogan, A. A., and Thorn, K. S. (1998) Anatomy of hot spots in protein interfaces. *J. Mol. Biol. 280*, 1–9.
(51) Lo Conte, L., Chothia, C., and Janin, J. (1999) The atomic structure of protein-protein recognition sites. *J. Mol. Biol. 285*, 2177–2198.
(52) Glaser, F., Steinberg, D. M., Vakser, I. A., and Ben-Tal, N. (2001) Residue frequencies and pairing preferences at protein-protein interfaces. *Proteins 43*, 89–102.
(53) Koide, S., and Sidhu, S. S. (2009) The importance of being tyrosine: lessons in molecular recognition from minimalist synthetic binding proteins. *ACS Chem. Biol. 4*, 325–334.
(54) Hajduk, P. J., Bures, M., Praestgaard, J., and Fesik, S. W. (2000) Privileged molecules for protein binding identified from NMR-based screening. *J. Med. Chem. 43*, 3443–3447.
(55) Nayal, M., and Honig, B. (2006) On the nature of cavities on protein surfaces: application to the identification of drug-binding sites. *Proteins 63*, 892–906.
(56) Pryor, K. E., Shipps, G. W., Skyler, D. A., and Rebek, J. (1998) The activated core approach to combinatorial chemistry: A selection of new core molecules. *Tetrahedron 54*, 4107–4124.
(57) Otwinowski, Z., and Minor, W. (1997) Processing of X-ray diffraction data collected in oscillation mode, in *Methods in Enzymology* (C.W. Carter, C. W., Jr., and Sweet, R. M., Eds.), pp 307−326, Academic Press, New York.
(58) Navaza, J. (1994) AMoRe: an automated package for molecular replacement. *Acta Crystallogr. A50*, 157–163.
(59) Brunger, A. T., Adams, P. D., Clore, G. M., DeLano, W. L., Gros, P., Grosse-Kunstleve, R. W., Jiang, J.-S., Kuszewski, J., Nilges, M., Pannu, N. S., Read, R. J., Rice, L. M., Simonson, T., and Warren, G. L. (1998) Crystallography & NMR system: A new software suite for macromolecular structure determination. *Acta Crystallogr. D: Biol. Crystallogr. 54*, 905–921.
(60) Vagin, A. A., Steiner, R. A., Lebedev, A. A., Potterton, L., McNicholas, S., Long, F., and Murshudov, G. N. (2004) REFMAC5 dictionary: organization of prior chemical knowledge and guidelines for its use. *Acta Crystallogr. D: Biol. Crystallogr. 60*, 2184–2195.
(61) Laskowski, R. A., MacArthur, M. W., Moss, D. S., and Thornton, J. M. (1993) PROCHECK: a program to check the stereochemical quality of protein structures. *J. Appl. Crystallogr. 26*, 283–291.